



# HOKKAIDO UNIVERSITY

Title	Crystallization and magnetic property of iron oxide nanoparticles precipitated in silica glass matrix
Author(s)	Masubuchi, Y.; Sato, Y.; Sawada, A. et al.
Citation	Journal of the European Ceramic Society, 31(14), 2459-2462 <a href="https://doi.org/10.1016/j.jeurceramsoc.2011.02.016">https://doi.org/10.1016/j.jeurceramsoc.2011.02.016</a>
Issue Date	2011-11
Doc URL	<a href="https://hdl.handle.net/2115/47352">https://hdl.handle.net/2115/47352</a>
Type	journal article
File Information	JECS31-14_2459-2462.pdf



Crystallization and Magnetic Property of Iron Oxide Nanoparticles Precipitated in Silica  
Glass Matrix.

Y. Masubuchi\*, Y. Sato, A. Sawada, T. Motohashi, H. Kiyono and S. Kikkawa

Affiliation;

Faculty of Engineering, Hokkaido University, N13-W8, Kita-ku, Sapporo, 060-8628, Japan

\*Corresponding author: Y. Masubuchi; address: Faculty of Engineering, Hokkaido University,

Sapporo 060-8628, Japan; Tel/Fax: +81-(0)11-706-6742/6740; E-mail:

yuji-mas@eng.hokudai.ac.jp

## Abstract

Crystallization and magnetic property of  $\text{Fe}_2\text{O}_3$  nanoparticle precipitated in  $\text{SiO}_2$  matrix was investigated.  $\text{Fe}_2\text{O}_3/\text{SiO}_2$  nanocomposite thin film was obtained by annealing of the amorphous Fe-Si-O thin film deposited by RF-magnetron sputtering of  $(\alpha\text{-Fe}_2\text{O}_3)_{1-x}/(\text{SiO}_2)_x$  composite targets. The  $\text{Fe}_2\text{O}_3$  crystallite size increased with decreasing  $\text{SiO}_2$  area ratio,  $x$  of the target and increasing annealing temperature.  $\epsilon\text{-Fe}_2\text{O}_3$  with the crystallite size of 20 ~ 30 nm was obtained after annealing the film deposited in  $\text{SiO}_2$  area ratio,  $x = 0.33 \sim 0.42$  at 900 °C. Lower  $\text{SiO}_2$  area ratio ( $x$ ) than 0.25 and higher annealing temperature resulted in precipitation of  $\alpha\text{-Fe}_2\text{O}_3$  with the larger crystallite size than 40 nm. In the case of  $\text{SiO}_2$  area ratio,  $x \geq 0.50$ , the annealed film was amorphous and showed higher magnetization and smaller coercivity due to the precipitation of very small crystalline  $\gamma\text{-Fe}_2\text{O}_3$ . The  $\epsilon\text{-Fe}_2\text{O}_3/\text{SiO}_2$  composite thin film showed ferromagnetic hysteresis with coercive force of 0.14 T.

## Keywords:

Iron oxide; Thin film; Nanocomposites; Magnetic properties; Thermal annealing;

## 1. Introduction

Iron (III) oxide ( $\text{Fe}_2\text{O}_3$ ) has four polymorphs:  $\alpha$ -,  $\beta$ -,  $\gamma$ -, and  $\epsilon$ - $\text{Fe}_2\text{O}_3$ <sup>1</sup>. The  $\alpha$ - and  $\gamma$ - $\text{Fe}_2\text{O}_3$  have been extensively studied for applications in non-toxic inorganic red pigment and magnetic recording media, respectively.  $\alpha$ -phase has a corundum structure and exhibits antiferromagnetic characteristic ( $T_N = 950$  K) with slightly canting in spins resulting in a weak ferromagnetism<sup>2,3</sup>.  $\gamma$ -phase has a spinel structure and ferrimagnetic behavior with a Curie temperature ( $T_C$ ) of  $928$  K<sup>1,4</sup>. Recently, an enormously large room temperature coercivity about  $2$  T was reported on  $\epsilon$ - $\text{Fe}_2\text{O}_3$  phase<sup>5-7</sup>, but the value is not reproducible<sup>8,9</sup>. It has an orthorhombic structure and is ferromagnetic with  $T_C = 480$  K<sup>6,10</sup>.  $\beta$ -phase is another new phase having a bixbyite structure and exhibits antiferromagnetic feature with a Neel temperature ( $T_N$ ) of  $119$  K<sup>11-13</sup>.  $\alpha$ - $\text{Fe}_2\text{O}_3$  is the thermodynamically most stable among these four polymorphs. Other  $\text{Fe}_2\text{O}_3$  polymorphs also appear in stabilizing by the surface energy of their particles in nanometer scale.  $\epsilon$ - $\text{Fe}_2\text{O}_3$  is a phase reported only as nanocomposites with  $\text{SiO}_2$  derived by polymerization of TEOS or triethoxysilane<sup>14,15</sup>. In this view point, M. Gich et al. have reported that the confinement of particle size in the  $\text{SiO}_2$  matrix plays an important role in the formation and stabilization of  $\epsilon$ - $\text{Fe}_2\text{O}_3$  and crystal structure change in the order of  $\gamma \rightarrow \epsilon \rightarrow \alpha$ - $\text{Fe}_2\text{O}_3$  as increase in the nanoparticle size<sup>16</sup>. Recently, the phase transformation among the four  $\text{Fe}_2\text{O}_3$  polymorphs has been proposed to be  $\gamma \rightarrow \epsilon \rightarrow \beta \rightarrow$

$\alpha$ -Fe<sub>2</sub>O<sub>3</sub> with increasing particle size using the impregnation method<sup>17</sup>. The  $\epsilon$ -Fe<sub>2</sub>O<sub>3</sub> particle size was in a range of 10 ~ 30 nm diameter in those reports.

These  $\epsilon$ -Fe<sub>2</sub>O<sub>3</sub>/SiO<sub>2</sub> nanocomposites have been synthesized by controlling Fe<sub>2</sub>O<sub>3</sub> particle size dispersed in SiO<sub>2</sub> matrix in various kinds of chemical route. Aqueous solution of Fe(NO<sub>3</sub>)<sub>2</sub> was hydrolyzed together with TEOS or triethoxysilane to be confined in silica gel<sup>6,10</sup>. Hydrolysis was also applied on Fe(III) complex with complicated ligands containing -Si(OCH<sub>3</sub>) bonds<sup>8</sup>. The droplet size of Fe solution was tried to control in several studies using reverse-micelle or impregnation into mesoporous SiO<sub>2</sub> particles<sup>5,9,17</sup>. It is obviously not easy to control the nanoparticle size in the sol-gel related routes because iron oxide easily precipitates outside SiO<sub>2</sub> matrix to aggregates in a large grain size to form the most stable  $\alpha$ -Fe<sub>2</sub>O<sub>3</sub> after their thermal treatment. This is the reason why the  $\epsilon$ -Fe<sub>2</sub>O<sub>3</sub>/SiO<sub>2</sub> composites contaminated with  $\alpha$ -Fe<sub>2</sub>O<sub>3</sub> impurity in most studies. Nano-sized magnetic alloy has been synthesized by simple thermal annealing of an appropriate amorphous film<sup>18-20</sup>. Its nanoparticles precipitate from the amorphous alloy matrix via thermal diffusion during the annealing. The particle size can be controlled in the precipitation only by changing the thermal annealing condition and the starting composition.

In this study, amorphous Fe-Si-O thin films deposited on a silica glass substrate by RF-magnetron sputtering were thermal annealed to precipitate  $\epsilon$ -Fe<sub>2</sub>O<sub>3</sub> nanoparticles in

SiO<sub>2</sub> matrix. The annealed thin films were investigated in their structure and magnetic property.

## 2. Experimental procedure

Silica glass chips (wedge shape with radius of 38 mm and inner angle of 30°) (99.99%, Kojyundo Chemical Laboratory Co.) were distributed on an  $\alpha$ -Fe<sub>2</sub>O<sub>3</sub> target (diameter of 76.2 mm) (99.9%, Kojyundo Chemical Laboratory Co.) in the composite targets. Their SiO<sub>2</sub> area ratio was varied from  $x = 0.25$  to  $0.5$  in  $(\alpha\text{-Fe}_2\text{O}_3)_{1-x}(\text{SiO}_2)_x$  by changing the number of the chips. RF-magnetron sputter equipment (JEOL, JEC-SP360M) was operated in 5.0 Pa of Ar (99.9995% purity). Films were deposited on SiO<sub>2</sub> glass substrate while applying a RF power of 100 W for 2.5 hours. The as-deposited thin films were annealed in a temperature range between 700 and 1000 °C in air for 100 min. To attain the fixed annealing duration, the films were placed and then taken out from a box furnace at the certain temperatures.

Crystalline phases were characterized using X-ray diffraction (XRD) with monochromatized Cu-K $\alpha$  radiation (Rigaku, Ultima IV). Magnetic hysteresis was studied in a field of up to 1.5 T at room temperature using a vibrating sample magnetometer (Riken Denshi, BHV-50). The film thickness was estimated by observing their cross section in

scanning electron microscopy (SEM) (JEOL, JSM-6390LV). The chemical compositions of the films were analyzed by fluorescent X-ray spectroscopy (XRF) (SII, SEA6000VX) in thin film FP mode. The microstructure of the annealed film was observed by using transmission electron microscope (TEM) (JEOL, JEM-2100F). The sample observed was a cross sectional thin slice finished by Ar ion beam thirlling.

### 3. Results and discussion

As-deposited films were amorphous independently on the film composition as shown in Fig. 1(a). Their film thickness was about 1, 0.9, 0.8 and 0.7  $\mu\text{m}$  for  $x = 0.25, 0.33, 0.42$  and  $0.50$ , respectively, and decreased against the  $\text{SiO}_2$  area ratio,  $x$  in the  $(\alpha\text{-Fe}_2\text{O}_3)_{1-x}(\text{SiO}_2)_x$  composite target. Their  $\text{Fe}_2\text{O}_3/\text{SiO}_2$  compositional ratio in the deposited films were also measured by using XRF to be 68/32, 60/40, 48/52 and 40/60 in at% for the films with  $x = 0.25, 0.33, 0.42$  and  $0.50$ , respectively. The film annealed at  $900\text{ }^\circ\text{C}$  was still amorphous at  $x = 0.5$  (Fig. 1(b)).  $\text{Fe}_2\text{O}_3$  appeared as metastable  $\epsilon$  phase at  $x = 0.42$  and  $0.33$  (Figs. 1(c) and (d)) and then changed to  $\alpha$  phase at  $x = 0.25$  (Fig. 1(e)). In higher  $\text{SiO}_2$  content,  $\text{Fe}_2\text{O}_3$  concentration was too thin to form its crystallite detectable in X-ray diffraction. The crystallite size grew with the increasing  $\text{Fe}_2\text{O}_3$  content in the film to crystallize in  $\epsilon$  and  $\alpha\text{-Fe}_2\text{O}_3$ . It was calculated to be 20, 25 and 40 nm by using Scherrer equation from a single

diffraction peak observed at  $2\theta \approx 33^\circ$  for the thin films at  $x = 0.42, 0.33$  and  $0.25$ , respectively. The crystallite sizes for  $\epsilon$  phase were almost comparable to value obtained by sol-gel methods<sup>5,6,16</sup>.

TEM image of the annealed film at  $x = 0.33$  shows dark grains of ca. 22 nm diameter in bright region as depicted in Fig. 2. The grain observed in TEM is almost similar to the crystallite size 25 nm of  $\epsilon$ -Fe<sub>2</sub>O<sub>3</sub> calculated from XRD (Fig. 1(d)). The dark grains and bright part might be  $\epsilon$ -Fe<sub>2</sub>O<sub>3</sub> and SiO<sub>2</sub> matrix, respectively. Composite of  $\epsilon$ -Fe<sub>2</sub>O<sub>3</sub> nanoparticle and amorphous SiO<sub>2</sub> matrix was successfully obtained by the simple thermal annealing of Fe-Si-O amorphous film.

Figure 3 shows the magnetization curves for the thin films as-deposited and annealed at 900 °C. Total Fe<sub>2</sub>O<sub>3</sub> contents in each film were calculated by using film thickness and Fe<sub>2</sub>O<sub>3</sub>/SiO<sub>2</sub> compositional ratio in the films to show the magnetization per Fe<sub>2</sub>O<sub>3</sub> weight in the figure. The as-deposited film was paramagnetic due to its amorphous structure. The annealed film at  $x = 0.50$  showed magnetization curve having the highest magnetization, although it was again amorphous in XRD. The annealed films crystallized in  $\epsilon$ -Fe<sub>2</sub>O<sub>3</sub> exhibited a larger magnetic coercive force and lower magnetization than the values for  $x = 0.50$ . The largest coercive force of 0.10 T was obtained in the annealed film at  $x = 0.33$ .  $\alpha$ -Fe<sub>2</sub>O<sub>3</sub> observed at  $x = 0.25$  showed a weak ferromagnetic hysteresis with very small

coercive force due to its slightly canting in spins, i.e. Dzyaloshinsky- Moriya interaction<sup>2,3</sup>. The magnetization has been reported to be 80, 15 and 1 emu/g for  $\gamma$ ,  $\epsilon$  and  $\alpha$ -Fe<sub>2</sub>O<sub>3</sub>, respectively<sup>5</sup>.  $\gamma$ -Fe<sub>2</sub>O<sub>3</sub> has been reported to be stabilized in the smallest particle size among Fe<sub>2</sub>O<sub>3</sub> phases<sup>16,17</sup>. The annealed film with  $x = 0.50$  showed the highest magnetization probably because  $\gamma$ -Fe<sub>2</sub>O<sub>3</sub> having a smaller crystallite size below detection limit in XRD crystallized in SiO<sub>2</sub> matrix forming nanocomposite. The crystal structures of the annealed films changed in the order of  $\gamma \rightarrow \epsilon \rightarrow \alpha$ -Fe<sub>2</sub>O<sub>3</sub> as the SiO<sub>2</sub> contents decrease with increasing in their crystallite size.

The size of Fe<sub>2</sub>O<sub>3</sub> nanoparticles precipitated in SiO<sub>2</sub> matrix also changes with the annealing temperature. Figure 4 depicts the annealing temperature dependence of the crystallite size obtained from the composite target of  $x = 0.33$ .  $\epsilon$ -Fe<sub>2</sub>O<sub>3</sub> with 20 to 25 nm in crystallite size was observed between 800 and 900 °C. Above 950 °C, the crystallite size steeply increased to over 50 nm at 1000 °C. As the crystallite size increased, crystal structure of the Fe<sub>2</sub>O<sub>3</sub> changed to  $\alpha$ -Fe<sub>2</sub>O<sub>3</sub> reported to be stabilized above 30 nm in crystallite size. Their coercive force increased with increase in their crystallite size up to annealing temperature of 900 °C. The magnetic coercive force decreased with the phase transformation to  $\alpha$ -Fe<sub>2</sub>O<sub>3</sub>. The crystallite size was successfully controlled by changing the annealing temperature, as well as changing the film composition. The present crystallite size

around 25 nm suitable to obtain  $\epsilon$ -Fe<sub>2</sub>O<sub>3</sub> was comparable to the previously reported value in the preparation of  $\epsilon$ -Fe<sub>2</sub>O<sub>3</sub> in SiO<sub>2</sub> matrix<sup>5,6,16</sup>.  $\beta$ -Fe<sub>2</sub>O<sub>3</sub> did not precipitate even as an impurity phase in this study.

Magnetic coercivity values were summarized against crystallite size of Fe<sub>2</sub>O<sub>3</sub> observed in any kinds among the present annealed films by changing either  $x$ -value or annealing temperature in Fig. 5. The smallest crystallite size observed in XRD was 20 nm for  $\epsilon$ -Fe<sub>2</sub>O<sub>3</sub>. The annealed thin film with lesser iron content was XRD amorphous as in Fig. 1(b) and showed the largest magnetization in Fig. 3. Ferrimagnetic  $\gamma$ -Fe<sub>2</sub>O<sub>3</sub> nanoparticles might precipitate in smaller size than 15 nm as X-ray amorphous as already suggested in phase transformation of Fe<sub>2</sub>O<sub>3</sub> particle size<sup>16,17</sup>. Between 15 and 30 nm, we could obtain  $\epsilon$ -Fe<sub>2</sub>O<sub>3</sub>/SiO<sub>2</sub> nanocomposite. In this region, the annealed film with crystallite size of 21 nm showed the highest coercive force of 0.14 T.  $\alpha$ -Fe<sub>2</sub>O<sub>3</sub> was observed above 30 nm crystallite size and it showed a small coercive force of around 0.01 T due to its weak ferromagnetism. The coercive force of 0.14 T in  $\epsilon$ -Fe<sub>2</sub>O<sub>3</sub>/SiO<sub>2</sub> composite film observed in this study is much suppressed in contrast to the reported value of 2 T<sup>5-7</sup>. Small coercivity in  $\epsilon$ -Fe<sub>2</sub>O<sub>3</sub>/SiO<sub>2</sub> nanocomposite was also reported by several groups<sup>8,9</sup>. The enormously large coercivity of  $\epsilon$ -Fe<sub>2</sub>O<sub>3</sub> was interpreted as mainly due to its large magnetocrystalline anisotropy ( $K \sim 10^6$  erg/cm<sup>3</sup>) and its appropriate particle size effect to suppress the movement of magnetic

domain wall. It is well known that magnetic material has a maximal coercive force when its particle size is in critical size at which magnetic domain structure changes from single- to multi-domain<sup>22,23</sup>. It is difficult to obtain the  $\epsilon$ -Fe<sub>2</sub>O<sub>3</sub>/SiO<sub>2</sub> nanocomposite thin film with very large coercivity in the present study because the discrepancy from the previous value is very large.

#### 4. Conclusions

Fe<sub>2</sub>O<sub>3</sub>/SiO<sub>2</sub> nanocomposite thin film was obtained by annealing of the amorphous Fe-Si-O thin film deposited by RF-magnetron sputtering of ( $\alpha$ -Fe<sub>2</sub>O<sub>3</sub>)<sub>1-x</sub>/(SiO<sub>2</sub>)<sub>x</sub> composite targets by changing their area ratio, x. The crystal structure and crystallite size were controlled by changing thermal annealing condition and Fe<sub>2</sub>O<sub>3</sub>/SiO<sub>2</sub> compositional ratio.  $\epsilon$ -Fe<sub>2</sub>O<sub>3</sub> with crystallite size of 20 ~ 30 nm was obtained by annealing the film deposited using the target of SiO<sub>2</sub> area ratio, x = 0.33 ~ 0.42 at 900 °C. Lower SiO<sub>2</sub> area ratio and higher annealing temperature led to increase the crystallite size to more than 40 nm resulting in the formation of  $\alpha$ -Fe<sub>2</sub>O<sub>3</sub> phase showing a weak ferromagnetism. The annealed thin film was amorphous in the case of SiO<sub>2</sub> area ratio, x > 0.50. It showed the magnetic hysteresis having the largest magnetization and the smallest coercivity among the present study probably because of the  $\gamma$ -Fe<sub>2</sub>O<sub>3</sub> precipitation in very small crystallite size. The

$\epsilon$ -Fe<sub>2</sub>O<sub>3</sub>/SiO<sub>2</sub> nanocomposite thin film showed ferromagnetic hysteresis with the largest coercivity of 0.14 T at the maximum among the present products. Precipitation of the Fe<sub>2</sub>O<sub>3</sub> in SiO<sub>2</sub> matrix from amorphous oxide thin film was successfully controlled by changing the annealing temperature and Fe<sub>2</sub>O<sub>3</sub>/SiO<sub>2</sub> compositional ratio.

## References

1. Zboril R., Mashlan M., and Petridis D., *Chem. Mater.*, 2002 **14** 969-982.
2. Dzyaloshinsky I., *J. Phys. Chem. Solids*, 1958 **4** 241-255.
3. Moriya T., *Phys. Rev.*, 1960 **120** 91-98.
4. Gilileo M.A., *Phys. Rev.*, 1958 **109** 777-781.
5. Jin J., Ohkoshi S., Hashimoto K., *Adv. Mater.*, 2004 **16** 48-51.
6. Kurmoo M., Rehspringer J.L., Hutlova A., D'Orleans C., Vilminot S., Estournes C., and Niznansky D., *Chem. Mater.*, 2005 **17** 1106-1114.
7. Tseng Y.C., Souza-Neto N.M., Haskel D., Gich M., Frontera C., Roig A., Veenendaal M., and Nogues J., *Phys. Rev. B*, 2009 **79** 094404.
8. Brazda P., Niznansky D., Rehspringer J.L., Vejparvova J.P., *J. Sol-Gel Sci. Technol.*, 2009 **51** 78-83.
9. Nakamura T., Yamada Y., and Yano K., *J. Mater. Chem.*, 2006 **16** 2417-2419.
10. Tronc E., Chaneac C., and Jolivet J.P., *J. Solid State Chem.*, 1998 **139** 93-104.
11. Ben-Der L., Fischbein E., and Kalman Z., *Acta Cryst. B*, 1976 **32** 667.
12. Svendsen M.B., *Naturwissenschaften*, 1958 **45** 542.
13. Ikeda Y., Takano M., and Bando Y., *Bull. Inst. Chem. Res. Kyoto Univ.*, 1986 **64** 249-258.
14. Chaneac C., Tronc E., and Jolivet J.P., *Nanostruct. Mater.*, 1995 **6** 715-718

15. Chaneac C., Tronc E., and Jolivet J.P., *J. Mater. Chem.*, 1996 **6** 1905-1911.
16. Gich M., Roig A., Taboada E., Molins E., Bonafos C., and Snoeck E., *Faraday Discuss.*, 2007 **136** 345-354.
17. Sakurai S., Namai A., Hashimoto K., and Ohkoshi S., *J. Am. Chem. Soc.*, 2009 **131** 18299-18303.
18. Long J., Laughlin D.E., and McHenry M.E., *J. Appl. Phys.*, 2008 **103** 07E708.
19. Trudeau M.L., *Mater. Sci. Eng. A.*, 1995 **204** 233-239.
20. Rivero G., Multigner M., Garcia J.M., Crespo P., and Hernando A., *J. Magn. Magn. Mater.*, 1998 **177-181** 119-120.
21. Blake R.L., Hessevick R.E., Zoltai T. and Finger L.W., *Am. Mineral.*, 1966 **51** 123-129.
22. Kittel C., *Phys. Rev.*, 1946 **70** 965-971.
23. Kneller E.F., and Luborsky F.E., *J. Appl. Phys.*, 1963 **34** 656-658.

## Figure captions

Fig. 1. XRD patterns for the as-deposited film at  $x = 0.33$  (a) and annealed thin films at 900 °C for 100 min at (b)  $x = 0.50$ , (c)  $x = 0.42$ , (d)  $x = 0.33$ , and (e)  $x = 0.25$  in  $(\text{Fe}_2\text{O}_3)_{1-x}(\text{SiO}_2)_x$  targets. Symbols  $\circ$  and  $\blacktriangledown$  represent diffraction peaks for  $\epsilon$ -  $\text{Fe}_2\text{O}_3$  and  $\alpha$ - $\text{Fe}_2\text{O}_3$ , respectively. Theoretical patterns are also shown in the bottom using literature values for  $\epsilon$ -  $\text{Fe}_2\text{O}_3$ <sup>10</sup> and  $\alpha$ - $\text{Fe}_2\text{O}_3$ <sup>21</sup>. The peak profile (peak positions and intensity ratio) of (c) and (d) corresponds to that of  $\epsilon$ -  $\text{Fe}_2\text{O}_3$ .

Fig. 2. TEM image of the film annealed at 900 °C for 100 min with  $x = 0.33$  in  $(\alpha\text{-Fe}_2\text{O}_3)_{1-x}(\text{SiO}_2)_x$  target.

Fig. 3. Magnetic hystereses of the as-deposited and annealed films. They were annealed at 900 °C for 100 min.

Fig. 4. Crystallite size and magnetic coercive force in the annealed films with  $x = 0.33$  against its annealing temperature. Open circle and triangle represent crystallite size and coercive force, respectively. Dashed line shows expected changing in crystallite size below 800 °C because of a smaller size under detection limit in XRD. Upper arrows indicate

observed crystalline  $\text{Fe}_2\text{O}_3$  phases.

Fig. 5. Coercive force against the crystallite size in the annealed thin films. The  $\epsilon$ - and  $\alpha$ - $\text{Fe}_2\text{O}_3$  phases were observed in crystallite size between 15 nm and 30 nm and above, respectively. The film was X-ray amorphous in the size below 15 nm.

Figure 1

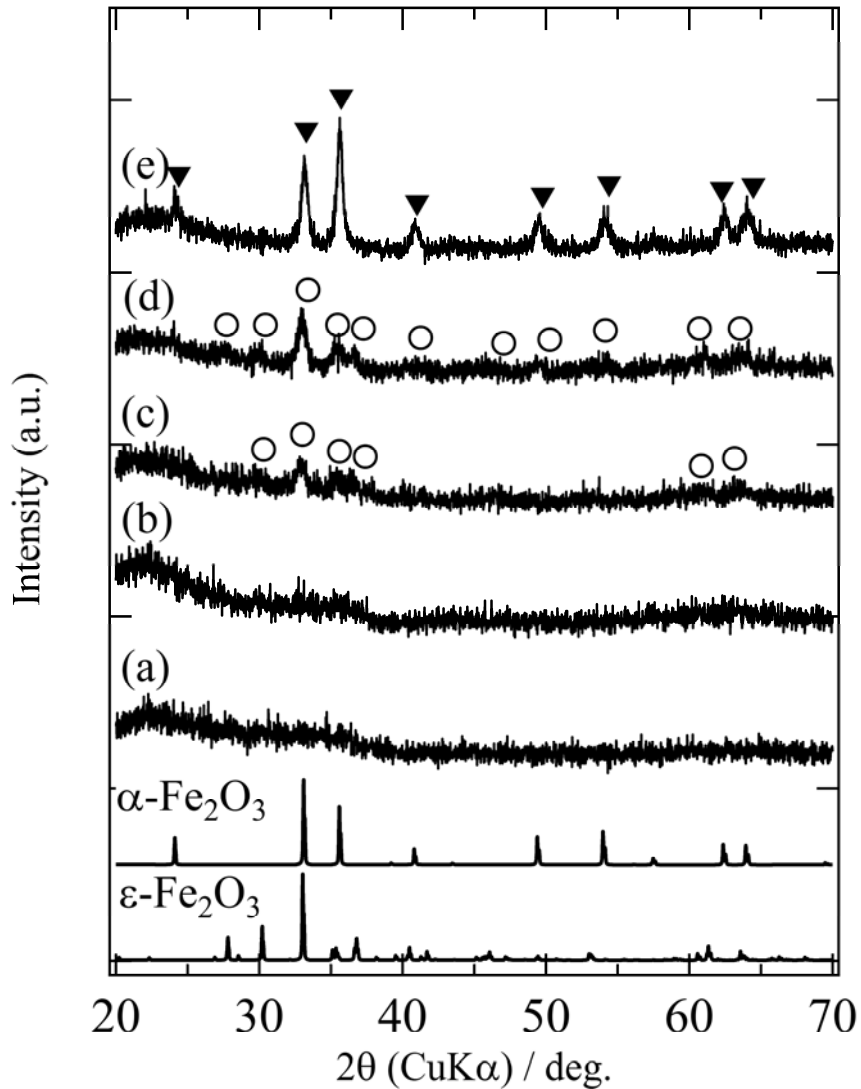


Fig. 1. XRD patterns for the as-deposited film at  $x = 0.33$  (a) and annealed thin films at  $900\text{ }^{\circ}\text{C}$  for 100 min at (b)  $x = 0.50$ , (c)  $x = 0.42$ , (d)  $x = 0.33$ , and (e)  $x = 0.25$  in  $(\text{Fe}_2\text{O}_3)_{1-x}(\text{SiO}_2)_x$  targets. Symbols  $\circ$  and  $\blacktriangledown$  represent diffraction peaks for  $\epsilon\text{-Fe}_2\text{O}_3$  and  $\alpha\text{-Fe}_2\text{O}_3$ , respectively. Theoretical patterns are also shown in the bottom using literature values for  $\epsilon\text{-Fe}_2\text{O}_3$ <sup>10</sup> and  $\alpha\text{-Fe}_2\text{O}_3$ <sup>21</sup>. The peak profile (peak positions and intensity ratio) of (c) and (d) corresponds to that of  $\epsilon\text{-Fe}_2\text{O}_3$ .

Figure 2

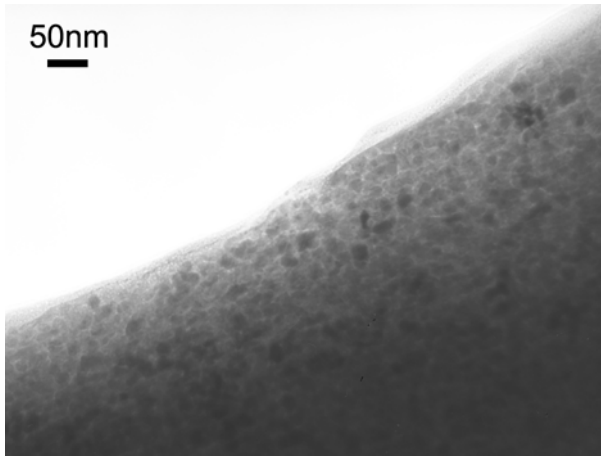


Fig. 2. TEM image of the film annealed at 900 °C for 100 min with  $x = 0.33$  in

$(\alpha\text{-Fe}_2\text{O}_3)_{1-x}(\text{SiO}_2)_x$  target.

Figure 3

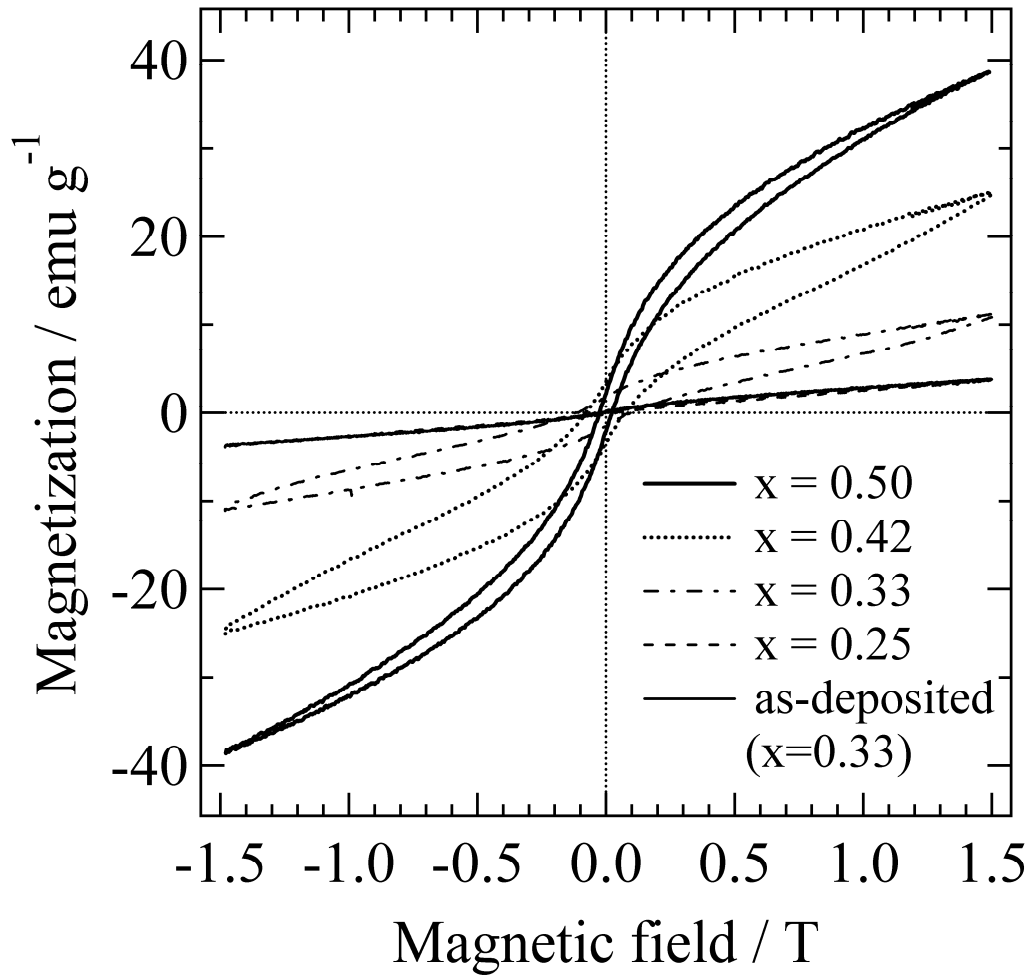


Fig. 3. Magnetic hystereses of the as-deposited and annealed films. They were annealed at

900 °C for 100 min.

Figure 4

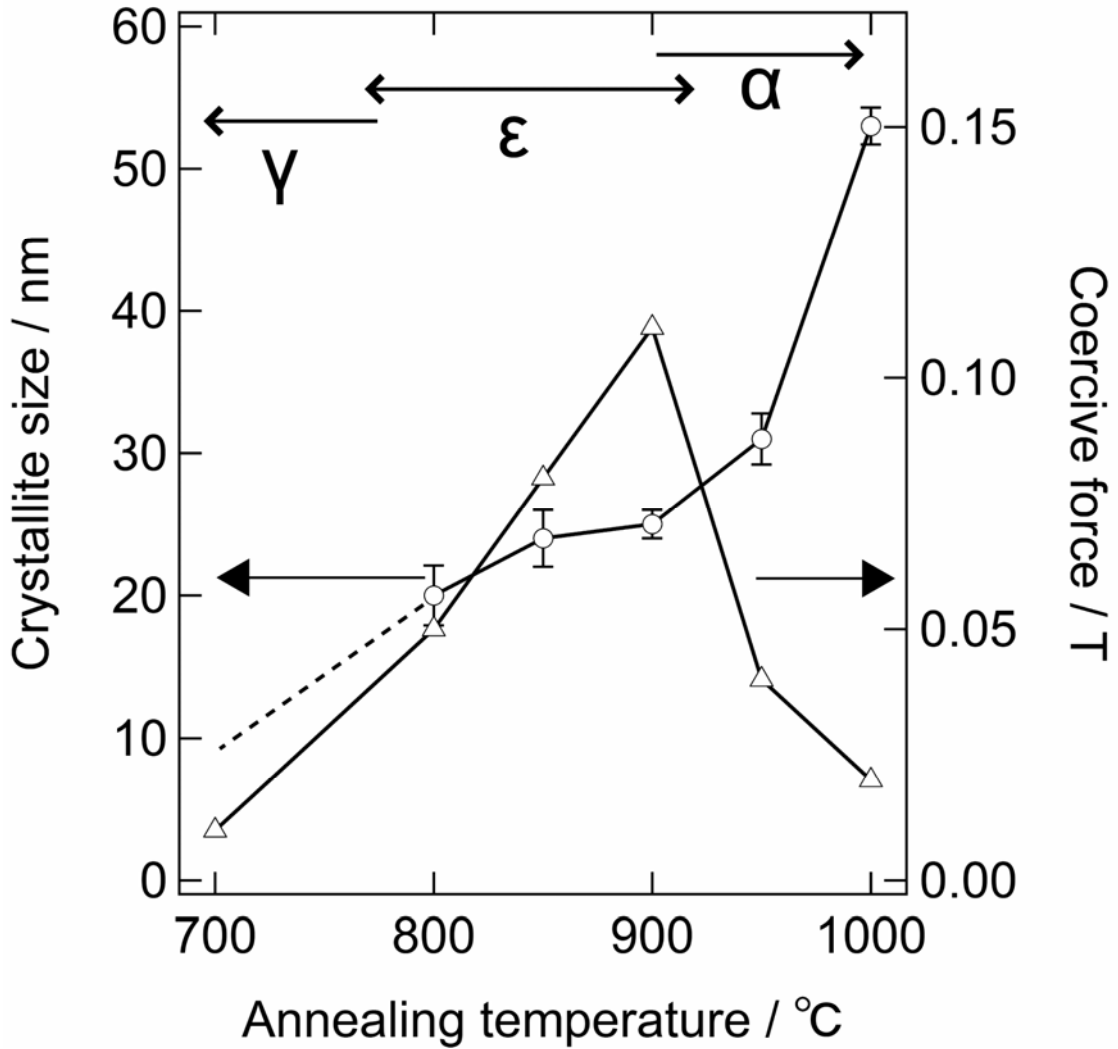


Fig. 4. Crystallite size and magnetic coercive force in the annealed films with  $x = 0.33$  against its annealing temperature. Open circle and triangle represent crystallite size and coercive force, respectively. Dashed line shows expected changing in crystallite size below 800 °C because of a smaller size under detection limit in XRD. Upper arrows indicate observed crystalline  $\text{Fe}_2\text{O}_3$  phases.

Figure 5

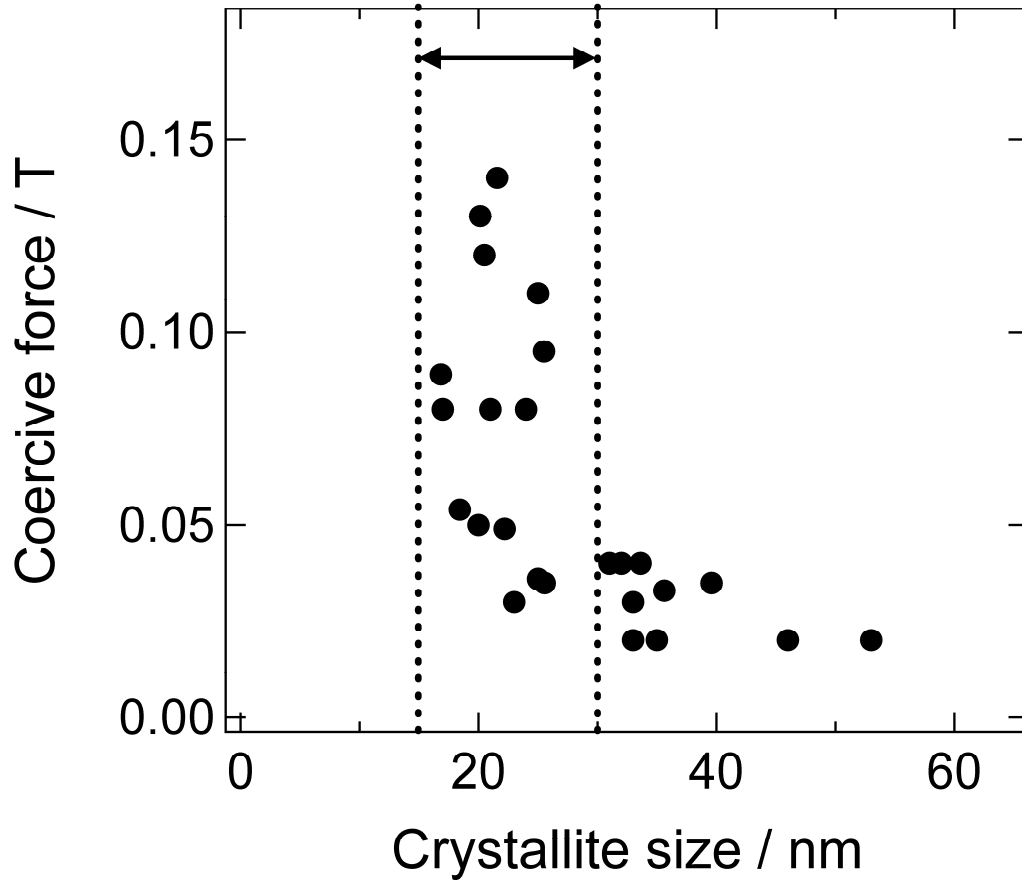


Fig. 5. Coercive force against the crystallite size in the annealed thin films. The  $\epsilon$ - and  $\alpha$ - $\text{Fe}_2\text{O}_3$  phases were observed in crystallite size between 15 nm and 30 nm and above, respectively. The film was X-ray amorphous in the size below 15 nm.